Contribution from the Laboratoire de Spectrochimie des Elêments de Transition, ERA No. 672, Université de Paris-Sud, 91405 Orsay, France, the Laboratoire de Chimie de Coordination du CNRS, Associeé à l'Université Paul Sabatier, 31400 Toulouse, France, and the Chemistry Department, University of Tasmania, Hobart, Tasmania 7001, Australia

Crystal Structure and Spectroscopic and Magnetic Properties of a Novel Nickel(II) Dimer Containing a Tridentate Nitrite Group: $[Ni(NH_2CH_2CH_2NH_2)_2NO_2]_2[B(C_6H_5)_4]_2$

A. GLEIZES,[1a] A. MEYER,[1b] M. A. HITCHMAN,[1c] and O. KAHN*[1b]

Received October 5, 1981

The title complex was synthesized and its crystal structure solved at 108 K. It crystallizes in the monoclinic system, space group $P2_1/n$. The lattice constants are $a = 16.571$ (6) Å, $b = 14.911$ (5) Å, $c = 11.117$ (2) Å, and $\beta = 104.02$ (2)° with $Z = 4$. Least-squares refinement of the structure has led to an R factor of 0.043. In contrast to the already known $[Ni(en)_2NO_2]X$ compounds, which are monomeric (X = Cl, Br, or I) or have a chain structure (X = ClO_4, BF_4, PF_6, or I_3), the structure of the title complex consists of asymmetric $[Ni(en)_2NO_2]_2^{2+}$ dimeric cations separated by tetraphenylborate counteranions. One nitrite in each dimer is tridentate, bridging the two nickel ions via a single oxygen atom while at the same time chelating to one nickel via the second oxygen atom. The second nitrite is bound as a monodentate nitrito group to the other nickel ion. The intramolecular Ni–Ni distance is 4.242 Å. The full refinement of the structure was particularly tedious owing to the disorder of the NO_2 groups, and the ultimate uncertainties on the coordination of these groups were removed by the study of the electronic absorption spectra. The magnetic behavior of the complex was studied in the 3.8–300 K temperature range and revealed an intramolecular antiferromagnetic coupling characterized by $J = -25.0$ cm^{-1}, the exchange Hamiltonian being $-J\hat{S}_1\cdot\hat{S}_2$. In spite of the shorter Ni–Ni distance, this coupling is weaker than that found in the $[Ni(en)_2NO_2]X$ chains. An explanation of this difference, based on the concept of magnetic orbitals, is proposed.

Introduction

The nitrite group is unusual because of the number of different ways in which it can coordinate to a metal.[2] As a monodentate ligand it can bond via either nitrogen or oxygen, while as a bidentate ligand it can chelate or bridge either via nitrogen and oxygen or via a single oxygen atom. In two compounds, $Cd(en)(NO_2)_2$,[3] en = 1,2-diaminoethane, and $K_2Pb(NO_2)_3NO_3\cdot H_2O$,[4] tridentate nitrite ligands occur, with these in each case being chelated to one metal ion and bridged to a second via nitrogen (shown by structure A). The factors

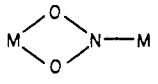

A

influencing the type of nitrite coordination adopted are often delicately balanced. For example, in a series of compounds of general formula $[Ni(en)_2NO_2]X$, chelating nitrite groups occur when X = Cl, Br, I, or NO_3,[5] while when X = ClO_4, BF_4, PF_6, or I_3[6,7] linear chains of nickel(II) ions occur, bridged by nitrite groups coordinated via nitrogen and oxygen (shown by structure B). Because of the versatility of the nitrite group

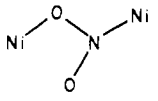

B

as a bridging ligand the study of polymeric nitrite complexes should provide useful information on the superexchange mechanisms operating in polymeric metal complexes. In a recent paper,[7] we have described the crystal structures and the magnetic properties of the compounds $[Ni(en)_2NO_2]X$ with X = ClO_4, BF_4, PF_6, or I_3. In these, the shortest intrachain Ni–Ni distance is relatively large, namely, 5.15 Å in the perchlorate compound. Nevertheless the magnetic properties reveal a strong intrachain antiferromagnetic coupling characterized by $J = -33.0$ cm^{-1}, the exchange Hamiltonian being defined by $-J\sum_i \hat{S}_i\hat{S}_{i+1}$. The mechanism of the exchange in these Ni(II) chains was interpreted with use of an orbital model proposed by one of us,[8] and predictions of the influence of the ONO angles of the bridging ligand were formulated. It was in order to check these predictions that we modified the nature of the X counteranion. Unfortunately, in all the cases where the chain structure is retained, the ONO angle remains practically unchanged. On the other hand, with the counteranion tetraphenylborate, BPh_4, we have obtained a novel compound of formula $[Ni(en)_2NO_2]BPh_4$, the structure of which is quite different, both from the above polymers and from the isolated $[Ni(en)_2NO_2]^+$ ions present when X = Cl, Br, I, or NO_3. It consists of asymmetric $[Ni(en)_2NO_2]_2^{2+}$ dimers in which the nickel(II) ions are bridged via one oxygen atom of a nitrite group. The second oxygen atom chelates to a nickel ion, making the nitrite tridentate. As far as we are aware this is the first reported example of a nitrite ion coordinated in this manner. The other nitrite group is bonded to the second nickel(II) as a monodentate nitrito group.

In this paper we describe the novel structure of this compound and also report its electronic spectrum, which proved quite important in removing the ultimate uncertainty of the crystal structure study. Indeed, we shall see that the refinement of the structure was particularly tedious owing to the disorder of the NO_2 groups. Finally, we give the magnetic properties of the compound, which show that the Ni(II) ions in the dimeric unit are antiferromagnetically coupled. However, this interaction is weaker than that in the $[Ni(en)_2NO_2]^+$ chains, in spite of the smaller Ni–Ni separation. An orbital interpretation of this difference is proposed.

Experimental Section

Synthesis. The preparation of $[Ni(en)_2NO_2]BPh_4$ (in fact $[Ni(en)_2NO_2]_2(BPh_4)_2$ as proved by the crystal structure) is carried out according to the reaction $[Ni(en)_2(H_2O)_2](BPh_4)_2 + NaNO_2 \rightarrow [Ni(en)_2NO_2]BPh_4 + NaBPh_4$. In order to avoid the formation of $[Ni(en)_3](BPh_4)_2$ from the equilibrium[9]

$$3[Ni(en)_2]^{2+} + 6H_2O \rightleftarrows 2[Ni(en)_3]^{2+} + [Ni(H_2O)_6]^{2+}$$

(1) (a) Laboratoire de Chimie de Coordination du CNRS. (b) Laboratoire de Spectrochimie des Elêments de Transition. (c) University of Tasmania.
(2) For a general discussion on the properties and structure of transition-metal nitrite complexes see: Hitchman, M. A.; Rowbottom, G. *Coord. Chem. Rev.* **1982**, *40*, 55.
(3) Shvelashvili, A. E.; Porai-Koshits, M. A. *Koord. Khim.* **1975**, *1*, 467.
(4) Nardelli, M.; Pelizzi, G. *Inorg. Chim. Acta* **1980**, *38*, 15.
(5) Shvelashvili, A. E.; Porai-Koshits, M. A.; Antisyshikima, A. S. *J. Struct. Chem. (Engl. Transl.)* **1965**, *6*, 155.
(6) Drew, M. G. B.; Goodgame, D. M. L.; Hitchman, M. A.; Rogers, D. *Chem. Commun.* **1965**, 477.
(7) Meyer, A.; Gleizes, A.; Girerd, J. J.; Verdaguer, M.; Kahn, O. *Inorg. Chem.* **1982**, *21*, 1729.
(8) Girerd, J. J.; Charlot, M. F.; Kahn, O. *Mol. Phys.* **1977**, *33*, 1063.

0020-1669/82/1321-2257$01.25/0

Table I. Experimental Crystallographic Data

(1) Physical and Crystallographic Data

formula: $Ni(N_2C_2H_8)_2(NO_2)(B(C_6H_5)_4)$
cryst syst: monoclinic
space group: $P2_1/n$
cell constants: at 293 K a = 16.714 (5) Å, b = 15.019 (2) Å, c = 11.287 (2) Å, β = 104.02 (2)°, V = 2749 Å^3; at 108 K a = 16.571 (6) Å, b = 14.911 (5) Å, c = 11.117 (2) Å, β = 104.40 (2)°, V = 2661 Å^3
mol wt: 544.152
ρ_{exptl}: was not measd
ρ_x(293 K) = 1.315 g cm^{-3}
Z = 4
morphology: face indices (0$\bar{1}$0), (0$\bar{1}$0), (1$\bar{1}$0), ($\bar{1}$10), (111), ($\bar{1}$1$\bar{1}$); dimens 0.22 × 0.36 × 0.52 mm
abs factor: $\mu_{MoK\alpha}$ = 7.64 cm^{-1}
transmission factors: min = 0.588, max = 0.866

(2) Data Collection

temp: 108 K
radiation: λ(Mo Kα) = 0.71069 Å
monochromatization: oriented graphite crystal
cryst-detector dist: 208 mm
detector window: height = 4 mm; width = 4 mm
takeoff angle: 3.4°
scan mode: θ-2θ
max Bragg angle: 2θ = 60°
scan angle: $\Delta\theta = \Delta\theta_0 + B \tan\theta$; $\Delta\theta_0$[a] = 0.75, B[a] = 0.347
values determining scan speed: SIGPRE[a] = 0.66, SIGMA[a] = 0.018, VPRE[a] = 10° min^{-1}, TMAX[a] = 60 s
std intens reflctns: 320, 600, 455 measd every 3600 s
independent recorded reflctns: 6356

[a] These parameters have been described in: Mosset, A.; Bonnet, J. J.; Galy, J. *Acta Crystallogr., Sect. B* 1977, *33*, 2633.

which is strongly displaced toward the right with the tetraphenylborate counteranion, we must work with a large excess of $[Ni(H_2O)_6]^{2+}$. We must also operate with a large excess of NO_2^- to substitute H_2O. This substitution, which occurs without breaking of the metal–oxygen bond,[10] is favored in the presence of H_2O. $[Ni(en)_2(H_2O)_2](BPh_4)_2 \cdot 2H_2O$ was prepared according to the method of Farago et al.[11] A 1-g quantity (1.2 × 10^{-3} mol) of $[Ni(en)_2(H_2O)_2](BPh_4)_2 \cdot 2H_2O$ and 0.28 g (1.2 × 10^{-3} mol) of $[Ni(H_2O)_6]Cl_2$ were dissolved in 30 mL of methanol. Then a solution of 0.16 g (2.3 × 10^{-3} mol) of $NaNO_2$ in 2 mL of water was added. Well-shaped dark blue single crystals were obtained by slow evaporation. Anal. Calcd for $NiC_{28}H_{36}N_5B_1O_2$: Ni, 10.80; C, 61.88; H, 6.62; N, 12.88; B, 1.99. Found: Ni, 10.8; C, 61.89; H, 6.60; N, 12.79; B, 2.09.

Crystal Structure Study and Data Collection. Preliminary precession photographs were taken with a single crystal mounted on Stoe camera, with use of Mo Kα radiation. The crystal was found to be monoclinic with space group $P2_1/n$.

The crystal was transferred to an Enraf-Nonius CAD-4 computer-controlled four-circle diffractometer and cooled down to 108 K. Accurate unit cell constants were derived from a least-squares refinement of the setting angles of 25 reflections. They are reported in Table I.

Intensities were measured for the forms hkl and $hk\bar{l}$. Reflections with 2$\theta \leq 60°$ were scanned as described in Table I, with use of graphite-monochromatized Mo Kα radiation. The intensities of the three standard reflections showed no systematic trends. The raw intensity data were corrected for Lorentz and polarization effects and assigned standard deviations calculated with a conventional ignorance factor p of 0.05.[12] It resulted in a set of 6356 independent reflections from which 6252 had $F_o^2 > 3F_o^2$, and these were corrected for absorption[12] and used in the refinement of structural parameters.

Structure Refinement. Refinement of the structure was effected by full-matrix least-squares techniques.[12] Throughout the refinement the function minimized was $\sum w(|F_o| - |F_c|)^2$ where $|F_o|$ and $|F_c|$ are the observed and calculated structure amplitudes and the weight w is $4F_o^2/\sigma^2F_o^2$. The reliability coefficients are defined as

$$R = \sigma(||F_o| - |F_c||)/\sum F \qquad R_w = (\sum w(|F_o| - |F_c|)^2/\sum wF_o^2)^{1/2}$$

The atomic scattering factors for nonhydrogen atoms and anomalous dispersion terms for the nickel atom are from the tabulation given by Cromer and Waber.[13] The atomic scattering factors used for hydrogen were those of Stewart et al.[13]

The position of the nickel atom was determined from the Patterson function and refined together with the scale factor. The ensuing Fourier synthesis permitted easy localization of the tetraphenylborate anion, the two chelated diaminoethane groups, and a chelated nitrite group. An isotropic refinement including the corresponding B, C, N, and O atoms and treating the C_6H_5 phenyl groups as idealized rigid bodies resulted in R = 0.12 and R_w = 0.20 for the 1990 reflections with (sin θ)/λ < 0.46.

While the thermal parameters of most atoms stabilized at about 2 Å^2, those of atoms O(2,1) and N(1,1) from the chelated nitrite amounted to about 8 Å^2. When included in the refinement, the occupancies of these two atoms reduced down to 0.5 and 0.6, respectively, along with a deflation of the corresponding isotropic B's. In the following cycles of refinement they were fixed at $^1/_2$ and the thermal parameters of the nickel atom and of the atoms of the diaminoethane groups were allowed to vary anisotropically. This model yielded R = 0.10 and R_w = 0.16 for the 4000 reflections with (sin θ)/λ < 0.58.

A subsequent difference Fourier map showed the following three kinds of significant peaks, in ascending order of importance: (i) peaks corresponding to the hydrogen atoms of the diaminoethane groups, which were included in the following least-squares calculations as fixed contributions with isotropic thermal parameters equal to those of atoms to which they are attached; (ii) peaks spread over the phenyl rings, which were removed later on when the phenyl carbon atoms were refined individually and anisotropically; (iii) peaks located around the nitrite ligand, which were considered as disordered positions of the remaining one-third of this ligand. A least-squares cycle in which the nonhydrogen atoms of the cation were treated as anisotropic scatterers, the nonhydrogen atoms of the anion were treated as individual isotropic scatterers, and all hydrogen atoms were treated as fixed contributors gave R = 0.083 and R_w = 0.136 for the whole set of data. The disorder at the nitrite ligand could not be resolved straightforwardly, and several attempts were necessary to reach a consistent, even if not fully satisfying, solution (see discussion below). The occupancies of the disordered positions were estimated from peak heights in the difference Fourier maps and then refined in one least-squares calculation before being set fixed in ensuing calculations. In the last cycle of refinement, the highest variable-shift/esd ratios were less than 70% for atoms O(1,1), O(1,2), N(1,1), N(2), and N(3,1) and less than 15% for the other atoms, and the reliability factors stabilized at R = 0.043 and R_w = 0.072 for the 4000 observations with $I > 3\sigma(I)$ and (sin θ)/λ < 0.58 and 349 variables. The error in an observation of unit weight was 2.55 e. A final difference Fourier map did not show any significant features. Refined parameters are listed in Table II.

Measurement of Spectra. The electronic spectrum of an arbitrary crystal face of the complex was measured at 295 and 7 K with a Cary 17 spectrophotometer with the electric vector of light along each extinction direction. The sample was masked with aluminum foil and cooled with a Cryodyne Model 21 cryostat. The lowering of the temperature served merely to sharpen the absorption bands somewhat.

Magnetic Measurements. These were performed in the 3.8–300 K temperature range with a previously described magnetometer on polycrystalline samples weighing about 5 mg. The magnetic fields were around 0.5 T. Tetrakis(thiocyanato)mercury cobaltate was used as a susceptibility standard. The diamagnetism was estimated as 720 × 10^{-6} cm^3 mol^{-1} and the TIP as 200 × 10^{-3} cm^3 mol^{-1} for $[Ni(en)_2NO_2]_2(BPh_4)_2$.

(9) Dwyer, F. P.; Gyarfas, E. C. *J. Proc. R. Soc. N.S.W.* **1949**, *83*, 232.
(10) Basolo, F.; Hammaker, G. S. *Inorg. Chem.* **1962**, *1*, 1.
(11) Farago, M. E.; James, J. M.; Trew, V. C. G. *J. Chem. Soc. A* **1967**, 820.
(12) All X-ray structure calculations were performed with use of the CII Iris-80 computer of the "Centre Interuniversitaire de Calcul de Toulouse". In addition to various local programs, modified versions of the following ones were employed: Ibers' AGNOST absorption program, which includes both the Coppens–Leiserowitz–Rabinovich logic for Gaussian integration and the Tompa analytical method; Zalkin's FORDAP Fourier summation program; Johnson's ORTEP thermal ellipsoid plotting program; Ibers' NUCL full-matrix least-squares program, which in its nongroup version resembles the Busing and Levy ORFLS program.
(13) Cromer, D. T.; Waber, J. T. "International Tables for X-ray Crystallography"; Kynoch Press: Birmingham, England, 1974; Vol. IV, Table 2.2A. Cromer, D. T. *Ibid.*, Table 2.3.1. Stewart, R. F.; Davidson, E. R.; Simpson, W. T. *J. Chem. Phys.* **1965**, *42*, 3175.

Table II. Positional and Thermal Parameters for the Atoms of $Ni(N_2C_2H_8)_2(NO_2)(B(C_6H_5)_4)$[a]

atom	mult	x	y	z	B_{11} or B_{iso}, Å^2	B_{22}	B_{33}	B_{12}	B_{13}	B_{23}
Ni	1	0.399 532 (19)	0.590 484 (21)	0.488 063 (28)	1.536 (15)	1.871 (16)	2.001 (16)	0.065 (10)	0.842 (12)	−0.301 (10)
O(1,1)	0.86	0.357 55 (22)	0.483 40 (20)	0.341 32 (28)	0.67 (13)	3.96 (14)	2.00 (11)	−0.67 (12)	0.28 (10)	0.16 (9)
O(2,1)	1/2	0.476 92 (22)	0.482 78 (24)	0.447 8 (3)	2.20 (15)	1.89 (15)	2.05 (13)	0.64 (12)	0.84 (11)	0.23 (11)
O(1,2)	0.14	0.390 4 (14)	0.488 2 (12)	0.369 7 (14)	1.41 (29)					
O(2,2)	0.14	0.324 9 (15)	0.406 3 (13)	0.261 7 (21)	5.8 (5)					
N(1,1)	1/2	0.417 9 (3)	0.449 5 (4)	0.360 7 (6)	1.79 (23)	2.40 (27)	2.24 (26)	0.41 (13)	0.95 (19)	0.47 (20)
N(2)	0.14	0.319 4 (17)	0.477 3 (16)	0.319 3 (20)	2.7 (4)					
N(2,1)	0.18	0.286 7 (8)	0.448 0 (8)	0.351 1 (11)	1.66 (19)					
N(3,1)	0.18	0.405 1 (10)	0.453 3 (11)	0.304 7 (14)	2.0 (3)					
N(1)E1	1	0.452 61 (17)	0.669 72 (18)	0.643 30 (22)	4.33 (13)	3.47 (12)	1.94 (9)	−1.52 (10)	−0.19 (9)	0.66 (9)
N(2)E1	1	0.362 89 (13)	0.512 43 (14)	0.619 65 (20)	2.25 (9)	1.58 (9)	2.31 (9)	0.24 (7)	0.80 (7)	−0.00 (7)
N(1)E2	1	0.286 15 (13)	0.658 32 (17)	0.437 82 (20)	1.53 (9)	3.35 (11)	2.30 (9)	0.27 (8)	0.62 (7)	0.88 (8)
N(2)E2	1	0.432 62 (14)	0.678 01 (15)	0.361 57 (20)	2.05 (9)	2.46 (10)	2.18 (9)	−0.20 (7)	1.11 (7)	−0.36 (8)
C(1)E1	1	0.442 09 (22)	0.624 59 (23)	0.758 36 (26)	4.20 (15)	3.59 (15)	1.88 (11)	−1.09 (13)	−0.11 (10)	0.51 (10)
C(2)E1	1	0.362 54 (17)	0.571 16 (18)	0.726 83 (24)	2.59 (12)	2.12 (11)	1.91 (10)	0.08 (9)	0.57 (9)	0.06 (9)
C(1)E2	1	0.285 27 (16)	0.708 98 (21)	0.323 52 (23)	1.99 (11)	3.58 (14)	1.87 (10)	0.18 (10)	0.47 (8)	0.67 (10)
C(2)E2	1	0.370 51 (17)	0.751 40 (19)	0.338 60 (23)	2.41 (11)	2.63 (12)	1.99 (10)	−0.12 (9)	0.99 (9)	0.20 (9)
B	1	0.105 73 (17)	0.734 26 (18)	0.637 89 (24)	1.34 (4)					
C(1)G1	1	0.178 69 (18)	0.850 50 (18)	0.517 27 (27)	2.18 (11)	1.55 (10)	3.35 (11)	0.42 (9)	1.62 (10)	0.45 (9)
C(2)G1	1	0.244 19 (22)	0.902 23 (18)	0.497 5 (3)	3.30 (15)	1.57 (11)	4.91 (17)	0.20 (10)	2.65 (14)	0.44 (11)
C(3)G1	1	0.319 63 (22)	0.901 70 (19)	0.585 1 (4)	3.34 (15)	1.68 (12)	6.07 (20)	−0.87 (10)	3.32 (15)	−1.07 (12)
C(4)G1	1	0.329 18 (19)	0.847 52 (22)	0.689 0 (3)	1.86 (12)	3.00 (14)	4.49 (16)	−0.67 (10)	1.32 (11)	−1.93 (12)
C(5)G1	1	0.262 68 (16)	0.794 69 (18)	0.705 90 (25)	1.43 (10)	1.83 (11)	2.71 (11)	−0.12 (8)	0.76 (9)	−0.74 (9)
C(6)G1	1	0.184 60 (15)	0.796 36 (16)	0.621 65 (24)	1.62 (10)	0.96 (9)	2.39 (10)	0.08 (8)	1.00 (8)	−0.30 (8)
C(1)G2	1	0.143 43 (16)	0.770 97 (18)	0.880 53 (24)	1.39 (10)	2.09 (11)	1.90 (10)	0.61 (8)	0.41 (8)	0.15 (9)
C(2)G2	1	0.138 77 (18)	0.757 28 (22)	0.002 71 (26)	2.39 (12)	3.37 (14)	1.92 (11)	1.39 (11)	0.29 (9)	−0.11 (10)
C(3)G2	1	0.098 90 (19)	0.684 11 (24)	0.032 83 (26)	3.12 (14)	3.95 (16)	1.89 (11)	1.51 (12)	1.06 (10)	0.90 (11)
C(4)G2	1	0.062 47 (20)	0.623 52 (22)	0.939 81 (29)	2.92 (15)	2.84 (14)	3.47 (14)	0.95 (11)	1.70 (12)	1.53 (12)
C(5)G2	1	0.067 00 (17)	0.637 44 (18)	0.817 70 (24)	0.05 (11)	1.96 (11)	2.14 (11)	0.33 (9)	0.96 (9)	0.54 (9)
C(6)G2	1	0.108 71 (14)	0.711 97 (17)	0.783 66 (22)	1.06 (9)	1.44 (10)	1.90 (10)	0.51 (8)	0.45 (8)	0.37 (8)
C(1)G3	1	0.005 69 (16)	0.879 47 (17)	0.596 90 (22)	1.63 (10)	1.57 (10)	1.28 (9)	0.15 (8)	0.41 (8)	0.06 (8)
C(2)G3	1	−0.072 43 (18)	0.919 63 (17)	0.568 34 (24)	2.24 (12)	1.87 (11)	1.51 (10)	0.64 (9)	0.58 (9)	0.20 (8)
C(3)G3	1	−0.144 27 (16)	0.867 66 (20)	0.533 46 (23)	1.69 (11)	2.88 (13)	1.69 (10)	0.74 (9)	0.41 (8)	0.34 (9)
C(4)G3	1	−0.135 79 (16)	0.774 75 (19)	0.524 59 (23)	1.70 (11)	0.58 (12)	1.62 (10)	0.02 (9)	0.44 (8)	0.31 (9)
C(5)G3	1	−0.057 53 (16)	0.736 11 (17)	0.551 65 (23)	1.61 (10)	1.54 (10)	1.68 (9)	−0.23 (8)	0.48 (8)	0.11 (8)
C(6)G3	1	0.016 38 (15)	0.785 79 (16)	0.589 46 (20)	1.50 (10)	1.41 (9)	1.08 (8)	0.00 (8)	0.54 (7)	0.14 (7)
C(1)G4	1	0.075 86 (17)	0.645 00 (18)	0.425 09 (23)	2.30 (12)	1.59 (10)	2.14 (11)	−0.38 (9)	1.08 (8)	−0.21 (9)
C(2)G4	1	0.081 96 (20)	0.572 45 (20)	0.349 46 (28)	3.24 (14)	2.16 (12)	2.45 (12)	−1.07 (11)	1.36 (10)	−0.59 (10)
C(3)G4	1	0.120 40 (19)	0.494 10 (19)	0.400 97 (29)	3.25 (14)	1.69 (11)	3.79 (14)	−0.84 (10)	2.15 (11)	−0.82 (10)
C(4)G4	1	0.151 94 (18)	0.489 37 (18)	0.528 95 (27)	2.35 (12)	1.25 (10)	3.49 (13)	−0.19 (9)	1.58 (10)	−0.06 (9)
C(5)G4	1	0.145 67 (16)	0.563 04 (18)	0.602 73 (25)	1.61 (10)	1.36 (10)	2.62 (11)	−0.15 (8)	0.95 (9)	0.01 (9)
C(6)G4	1	0.107 88 (15)	0.643 79 (17)	0.553 61 (24)	1.12 (9)	1.36 (10)	2.17 (10)	−0.30 (8)	0.84 (8)	−0.06 (8)

[a] Estimated standard deviations in the least significant figure(s) in this and subsequent tables are given in parentheses. The form of the anisotropic thermal ellipsoid is $\exp[-[^1/_4(B_{11}h^2a^{*2} + B_{22}k^2b^{*2} + B_{33}l^2c^{*2} + 2B_{12}hka^*b^* + 2B_{13}hla^*c^* + 2B_{23}klb^*c^*)]]$.

Description and Discussion of the Structure and Spectral Properties of the Complex

The complex consists of dimeric $[Ni(en)_2(NO_2)_2]_2^{2+}$ units with BPh_4^- counteranions. Important bond lengths and angles are listed in Table III, and the structure of the dimer together with the labeling of the atoms is shown in Figure 1. Each nickel(II) in the dimer is coordinated to two well-defined diaminoethane groups in a cis arrangement. The distorted-octahedral ligand coordination geometry of one nickel(II) is completed by a chelating nitrite (arrangement a in Figure 1), one oxygen of which bridges to the neighboring nickel(II). This tridentate nitrite coordination, which apparently has not been observed previously, is a combination of chelation, which occurs in several compounds of the type $[Ni(diamine)_2(NO_2)]X$,[5,14,15] and bridging via a single oxygen atom such as is found in several polymers of the form $[Ni(py)_2(NO_2)_2]_n$[16,17] and in the pentamer $Ni_5(N,N\text{-}Me_2en)_8(OH)_2(NO_2)_8$.[18] It is analogous to the tridentate coordination observed in certain carbonylate complexes:[19]

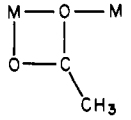

The Ni–Ni separation of 4.24 Å in the present dimer is somewhat greater than that of ~3.5 Å in the polymers containing single-oxygen-bridged nitrite groups.[17] This may well be due to the fact that each of the latter compounds contain ring systems of the form

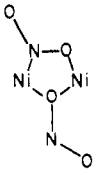

in which the angle ONiO is considerably less than that in the present compound (120° compared with 145°). As discussed

(14) Finney, A. J.; Hitchman, M. A.; Raston, C.; Rowbottom, G.; White, A. *Aust. J. Chem.*, in press.
(15) Birdy, R.; Goodgame, D. M. L.; McConway, J. C.; Rogers, D. *J. Chem. Soc., Dalton Trans.* **1977**, *18*, 1730.
(16) Goodgame, D. M. L.; Hitchman, M. A.; Marsham, D. F.; Phavanantha, P.; Rogers, D. *J. Chem. Soc. D* **1969**, 1382.
(17) Finney, A. J.; Hitchman, M. A.; Raston, C. L.; Rowbottom, G. L.; White, A. H. *Aust. J. Chem.* **1981**, *34*, 2125.
(18) Finney, A. J.; Hitchman, M. A.; Raston, C. L.; Rowbottom, G. L., White, A. H. *Aust. J. Chem.* **1981**, *34*, 2139.
(19) Deacon, G. B.; Phillips, R. J. *Coord. Chem. Rev.* **1980**, *33*, 227.

Table III. Relevant Bond Lengths (Å) and Angles (Deg) in $Ni(N_2C_2H_8)_2(NO_2)(B(C_6H_5)_4)$[a]

$[Ni(N_2C_2H_8)_2(NO_2)]_2^{2+}$ Cation

Arrangements a + b + c + d

Ni-N(1)E1	2.0956 (23)	N(1)E1-Ni-N(2)E1	82.65 (9)	Ni-N(1)E1-C(1)E1	109.68 (19)
Ni-N(2)E1	2.0750 (22)	N(1)E1-Ni-N(1)E2	96.48 (11)	Ni-N(2)E1-C(2)E1	107.23 (15)
Ni-N(1)E2	2.0841 (22)	N(1)E1-Ni-N(2)E2	94.33 (8)	Ni-N(1)E2-C(1)E2	107.13 (16)
Ni-N(2)E2	2.0892 (22)	N(2)E1-Ni-N(1)E2	93.37 (9)	Ni-N(2)E2-C(2)E2	106.88 (15)
N(1)E1-C(1)E1	1.493 (4)	N(2)E1-Ni-N(2)E2	175.39 (10)	N(1)E1-C(1)E1-C(2)E1	108.73 (22)
N(2)E1-C(2)E1	1.480 (3)	N(1)E2-Ni-N(2)E2	83.48 (9)	C(1)E1-C(2)E1-N(2)E1	108.79 (23)
N(1)E2-C(1)E2	1.475 (3)			N(1)E2-C(1)E2-C(2)E2	107.97 (20)
N(2)E2-C(2)E2	1.480 (3)			C(1)E2-C(2)E2-N(2)E2	107.39 (22)
C(1)E1-C(2)E1	1.505 (4)				
C(1)E2-C(2)E2	1.518 (4)				

Arrangements a + c + d

Ni-O(1,1)	2.265 (4)	O(1,1)-Ni-N(1)E1	168.89 (11)	O(1,1)-Ni-N(1)E2	93.11 (10)
		O(1,1)-Ni-N(2)E1	91.21 (8)	O(1,1)-Ni-N(2)E2	92.32 (9)

Arrangements b + c + d

Ni-O(2,1)^i	2.273 (3)	O(2,1)^i-Ni-N(1)E1	81.47 (12)	O(2,1)^i-Ni-N(1)E2	177.34 (15)
		O(2,1)^i-Ni-N(2)E1	84.71 (10)	O(2,1)^i-Ni-N(2)E2	98.33 (11)
				Ni-O(2,1)^i-Ni^i	145.39 (16)

Arrangements c + d

O(1,1)-Ni-O(2,1)^i	88.78

Arrangement a Only

Ni-O(2,1)	2.170 (3)	Ni-O(1,1)-N(1,1)	94.7 (5)	O(2,1)-Ni-N(1)E1	116.01 (12)
O(1,1)-N(1,1)	1.093 (6)	Ni-O(2,1)-N(1,1)	93.6 (3)	O(2,1)-Ni-N(2)E1	91.26 (11)
O(2,1)-N(1,1)	1.292 (7)	O(1,1)-N(1,1)-O(2,1)	117.1 (7)	O(2,1)-Ni-N(1)E2	147.50 (11)
		O(1,1)-Ni-O(2,1)	54.63 (12)	O(2,1)-Ni-N(2)E2	93.20 (11)

Arrangement b Only

Ni-O(1,2)	1.996 (17)	Ni-O(1,2)-N(2)	108.7 (21)	O(1,2)-Ni-N(1)E1	157.1 (7)
O(1,2)-N(2)	1.183 (28)	O(1,2)-N(2)-O(2,2)	99.6 (24)	O(1,2)-Ni-N(2)E1	92.8 (5)
N(2)-O(2,2)	1.252 (28)	O(1,2)-Ni-O(2,1)^i	75.8 (7)	O(1,2)-Ni-N(1)E2	106.2 (7)
				O(1,2)-Ni-N(2)E2	91.3 (5)

Arrangement c Only

O(1,1)-N(2,1)	1.316 (13)	Ni-O(1,1)-N(2,1)	110.1 (5)

Arrangement d Only

O(1,1)-N(3,1)	1.071 (16)	Ni-O(1,1)-N(3,1)	116.5 (9)

$B(C_6H_5)_4^-$ Anion

Around B Atom

B-C(6)G1	1.648 (4)	C(6)G1-B-C(6)G2	113.1 (3)	C(6)G2-B-C(6)G3	102.8 (4)
B-C(6)G2	1.643 (4)	C(6)G1-B-C(6)G3	112.2 (3)	C(6)G2-B-C(6)G4	113.3 (3)
B-C(6)G3	1.636 (4)	C(6)G1-B-C(6)G4	105.5 (3)	C(6)G3-B-C(6)G4	110.1 (3)
B-C(6)G4	1.648 (4)				

In Phenyl Rings

	ring G1	ring G2	ring G3	ring G4		ring G1	ring G2	ring G3	ring G4
C(1)-C(2)	1.393 (4)	1.395 (3)	1.390 (4)	1.389 (4)	C(6)-C(1)-C(2)	123.69 (28)	123.10 (26)	122.39 (24)	122.91 (26)
C(2)-C(3)	1.380 (5)	1.360 (5)	1.392 (4)	1.385 (4)	C(1)-C(2)-C(3)	119.36 (29)	120.34 (25)	120.48 (24)	120.14 (28)
C(3)-C(4)	1.387 (5)	1.393 (4)	1.398 (4)	1.390 (4)	C(2)-C(3)-C(4)	119.14 (27)	119.03 (19)	118.50 (24)	118.88 (25)
C(4)-C(5)	1.405 (4)	1.394 (4)	1.383 (4)	1.390 (4)	C(3)-C(4)-C(5)	120.48 (29)	120.54 (28)	120.17 (24)	119.98 (25)
C(5)-C(6)	1.396 (4)	1.409 (4)	1.403 (4)	1.404 (4)	C(4)-C(5)-C(6)	121.82 (27)	121.87 (28)	123.15 (24)	122.66 (25)
C(6)-C(1)	1.397 (4)	1.399 (4)	1.413 (3)	1.395 (3)	C(5)-C(6)-C(1)	115.43 (23)	115.12 (23)	115.28 (22)	115.40 (23)

[a] The roman numeral superscript i refers to the equivalent position $1-x, 1-y, 1-z$ relative to x, y, z as given in Table II.

in the section describing the crystal structure determination, the space-group requirements mean that the dimer is situated on a crystallographic inversion center, so that the nitrite groups are disordered. The tridentate form is made up of atoms O(1,1), N(1,1), and O(2,1), and its probability of occurrence is 0.5 per dimer. The second nitrite is bound as a monodentate ligand via oxygen, and the refinement of this group presented special problems as it was disordered not only across the inversion center of the dimer but also over three positions corresponding to different minima in a rotation about the Ni–O bond axis. These nitrito forms start either at atom O(1,2) (arrangement b) or at atoms O(1,1) (arrangements c and d). The former arrangement also contains atoms N(2) and O(2,2), and its probability of occurrence was found to be 0.14. The latter forms could not be fully characterized since although their nitrogen atoms were localized (N(2,1) for (c) and N(3,1) for (d)), their terminal oxygen atoms were not. In the refinement they were given equal probabilities of occurrence (found equal to 0.18) from the equality of height of the peaks attributed to N(2,1) and N(3,1) in the relevant difference Fourier map. The observed distances O(1,1)–N(1,1) = 1.093 (6) Å; O(1,1)–N(2,1) = 1.32 (1) Å, and O(1,1)–N(3,1) = 1.07 (2) Å are slightly out of the range 1.15–1.25 Å usually observed for N–O bonds in NO_2^- either as a bidentate or as a monodentate ligand.[2] Moreover the ellipsoid of O(1,1) was found to be more anisotropic than those of the other atoms. As a matter of fact the position of O(1,1) is most likely the mean position of two or three oxygen atoms very close to one another. Attempts to distinguish them in the refinement resulted in improved N–O bond lengths but never yielded convergence and therefore were given up. It is to be noted that the terminal oxygen atom of a nitrito group is frequently poorly

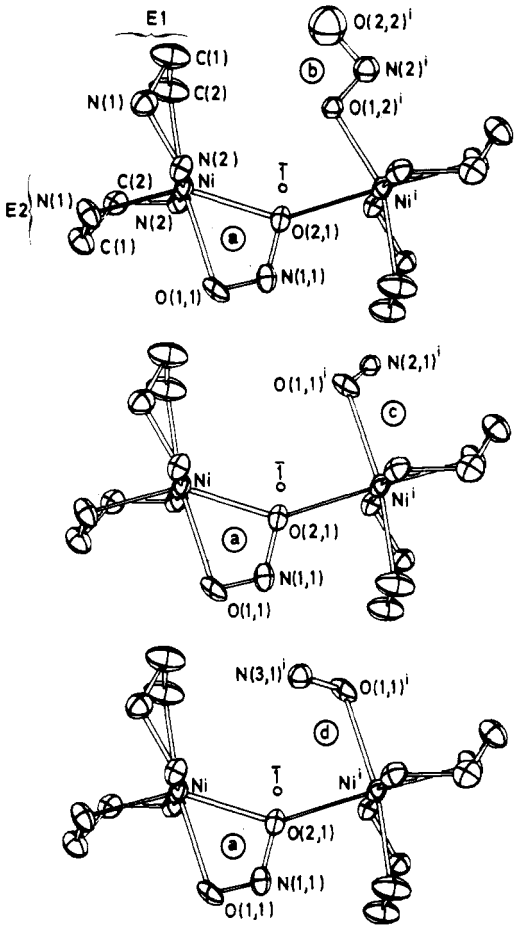

Figure 1. ORTEP drawings illustrating the molecular structure of the dimeric cation $[Ni(en)_2NO_2]_2^{2+}$ with the three possible arrangements (ab, ac, and ad) of the NO_2 group (see text and Table III). The atoms are drawn at their 50% probability ellipsoids. $\bar{1}$ is a crystallographic center of inversion.

resolved in crystal structure determinations, and such groups are often disordered about the metal–oxygen bond direction.[2] For instance, a 4-fold disorder occurs in $Ni(2\text{-MeIm})_4(ONO)_2$,[20] while a disorder over two different types of nitrito groups, one exhibiting a 2-fold rotational disorder, has been observed in $Ni(pyrazole)_4(ONO)_2$.[21]

Other possibilities for arrangements c and d were considered. In particular, the positions attributed to N(2,1) and N(3,1) could be due to the oxygen atoms of a nitro group whose nitrogen would be very near to O(1,1). This would not be inconsistent with the observed bond lengths and angles. The choice of two disordered nitrito groups instead of a nitro group was made largely on the basis of the electronic spectra. Electronic spectra of nickel(II) complexes containing monodentate and bridging

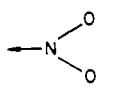

groups invariably show a strong absorption in the region 19 600–12 000 cm^{-1}.[2] Recent works suggest that this is probably a weak metal → nitrite charge-transfer transition, which is apparently characteristic of nitrite bound to nickel(II) via nitrogen.[2,22,23] Thus, the spectra of nickel(II) complexes

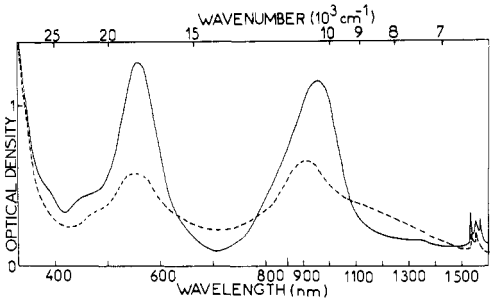

Figure 2. Electronic spectrum of an arbitrary crystal face of $[Ni(en)_2NO_2]_2(BPh_4)_2$ measured at 7 K with the electric vector of light along each of the two extinction directions.

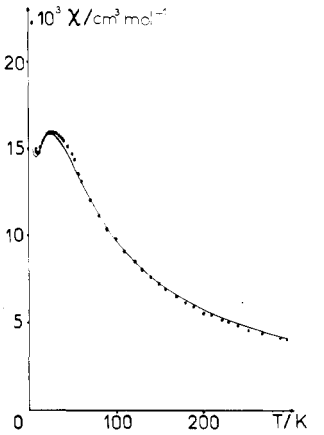

Figure 3. Experimental (●) and theoretical (—) thermal variations of the average magnetic susceptibility of $[Ni(en)_2NO_2]_2(BPh_4)_2$.

in which the metal is coordinated simultaneously to both a nitro and a nitrito group such as occurs in $Ni(isoquinoline)_4(NO_2)_2$[24] and solutions of $Ni(N,N\text{-}Me_2en)_2(NO_2)_2$[25] always show two peaks, one centered at ~20 000 cm^{-1} and the other ~17 500 cm^{-1}, due to the second spin-allowed d–d transition. In the spectrum of the present complex (Figure 2) no peak is observed at ~20 000 cm^{-1}. The spectrum is, in fact, essentially identical with those reported for single crystals of several compounds of the type $[Ni(diamine)_2(NO_2)]X$,[14,26] which show peaks at ~10 800 and 17 800 cm^{-1} with a weaker band at ~22 000 cm^{-1} and in which the nickel(II) is surrounded by four amine nitrogen atoms and two oxygens from a chelating nitrite; it is also identical with the spectrum of $[Ni(en)_2NO_2]NO_3$, which has a similar ligand arrangement.[5] the weak band at ~22 000 cm^{-1} is unusual, and this has been assigned as a spin-forbidden internal nitrite transition and is thought to be characteristic of nitrite ions chelated to nickel(II).[26] The electronic spectrum thus provides rather strong circumstantial evidence for a ligand coordination geometry involving four amine nitrogen and two cis oxygen atoms in agreement with the proposed structure. The infrared spectrum of the complex was also recorded and compared with those of $NaBPh_4$ and $[Ni(en)_2Cl]_2Cl_2$ in the hope that the nitrite peaks could be identified and used to elucidate the structure. However, the complexity of the spectra made a definitive assignment of the nitrite peaks impossible.

The geometry of the tetraphenylborate ion is unexceptional; the angles centered at the B-bonded carbon atoms (115.1 (2)–115.4 (2)°) are systematically smaller than those at the ortho positions, which are significantly larger than 120° (121.8 (3)–123.7 (3)°). The remaining angles do not depart sig-

(20) Finney, A. J.; Hitchman, M. A.; Raston, C. L.; Rowbottom, G. L.; White, A. H. *Aust. J. Chem.* **1981**, *34*, 2113.
(21) Finney, A. J.; Hitchman, M. A.; Raston, C. L.; Rowbottom, G. L.; White, A. H. *Aust. J. Chem.* **1981**, *34*, 2095.
(22) Hitchman, M. A.; Rowbottom, G. *Inorg. Chem.* **1982**, *21*, 823.
(23) Finney, A. J.; Hitchman, M. A.; Raston, C. L.; Rowbottom, G. L.; White, A. H. *Aust. J. Chem.* **1981**, *34*, 2085.
(24) Goodgame, D. M. L.; Hitchman, M. A. *Inorg. Chim. Acta* **1969**, *3*, 319. Hitchman, M. A.; Ahsbahs, H. *Inorg. Chim. Acta* **1981**, *53*, L97.
(25) Alexander, R. D.; Holper, P. N.; *Inorg. Nucl. Chem. Lett.* **1978**, *14*, 309 and references therein.
(26) Walker, I. M.; Lever, A. B. P.; McCarthy, P. J. *Can. J. Chem.* **1980**, *58*, 823.

nificantly from 120°, ranging from 118.5 (3) to 120.5 (3)°. This trend has been observed in other structures.[27]

Magnetic Results and Interpretation

All the attempts to grow single crystals of good quality with a size suitable for magnetic anisotropy measurements were unsuccessful. We needed crystals weighing at least 2 or 3 mg whereas the obtained crystals weighed less than 1 mg. The temperature dependence of the average molar susceptibility χ_M is shown in Figure 3. When the compound cools from room temperature, χ_M increases and reaches a rather broad maximum around 25 K, then decreases, and finally increases again below 9 K. The maximum of the χ_M vs. T plot is characteristic of an intramolecular antiferromagnetic coupling, and the behavior below 9 K is most likely due to uncoupled Ni(II) as an impurity. Since the coupling is antiferromagnetic with separations of several tens of wavenumbers between the low-lying spin states (see below), a small removal of the degeneracy of the excited spin triplet and spin quintet due to zero-field splitting will have a very weak influence on the magnetic behavior.[28] The zero-field splitting in the monomeric complexes $[Ni(en)_2(NO_2)]X$, X = Cl, Br, I, NO_3, is known to be quite small.[29] Since the energy parameters characterizing this splitting cannot be determined unequivocably from magnetic data obtained form polycrystalline samples,[29,30,31] this will be neglected in the following discussion. As the dimeric unit in $[Ni(en)_2NO_2]_2(BPh_4)_2$ is asymmetric, the g factors for each nickel(II) may be different.[32] Let us call these g_1 and g_2 and assume them to be isotropic. The spin Hamiltonian in the presence of a magnetic field H may be written as

$$H = (g_1\hat{S}z_1 + g_2\hat{S}z_2)\cdot\beta H - J\hat{S}_1\cdot\hat{S}_2 \qquad (1)$$

with an obvious meaning for the spin operators. The magnetic susceptibility χ_M^D for the asymmetric unit may be derived from (1) by using the Van Vleck relationship. This led to

$$\chi_M^D = \frac{2N\beta^2g^2}{kT}\frac{\exp(J/kT) + 5\exp(3J/kT)}{1 + 3\exp(J/kT) + 5\exp(3J/kT)} + \frac{2N\beta^2\delta^2}{3J}\frac{-8 + 3\exp(J/kT) + 5\exp(3J/kT)}{1 + 3\exp(J/kT) + 5\exp(3J/kT)} \qquad (2)$$

with

$$g = (g_1 + g_2)/2 \qquad \delta = (g_1 - g_2)/2$$

and the usual meanings for the constants N, β, and k. The second term in the expression of χ_M^D in (2) arises from the second-order coupling of the components of same M_s belonging to different spin states. In fact, this term plays a significant part only at very low temperatures, i.e., when the intrinsic susceptibility of the dimeric unit is hidden by the susceptibility of the uncoupled Ni(II) impurity. To account for this impurity, we expressed the observed susceptibility by

$$\chi_M = \chi_M^D(1 - \rho) + \frac{2N\beta^2g^2}{3kT}\rho \qquad (3)$$

ρ is the proportion of monomeric impurity, of which the susceptibility is assumed to follow a Curie law. Least-squares fitting with $\delta = 0$ led to the following values for the J, g, and ρ parameters:

$$J = -25.0\ cm^{-1} \qquad g = 2.23 \qquad \rho = 0.08$$

The agreement factor defined as $\sum(\chi_M(obsd) - \chi_M(calcd))^2/\sum(\chi_M(obsd))^2$ is then equal to 3×10^{-4}. The agreement is not improved in including $|\delta| \leq 0.3$ in the fitting procedure.

It has been shown that the exchange interaction parameter between nearest-neighbor ions M in the chain $(-M-X-M-X-)_n$ is expected to be equal to the exchange interaction parameter in the hypothetical dimer X-M-X-M-X.[8] In other words, the J values for a chain and a dimer with transition-metal ions of the same nature may be directly compared. It turns out that the Ni(II) ions are more weakly coupled in the dimeric unit $[Ni(en)_2NO_2]_2^{2+}$ than in the chains present in $[Ni(en)_2NO_2]X$, X = ClO_4, BF_4, PF_6, or I_3.[7] The J values are respectively −25.0 and −33.0 cm^{-1}. This difference is noticeable, especially as the distance between the interacting ions is significantly shorter in the dimer than in the chain, (4.24 Å compared with 5.15 Å). The low symmetry of the dimeric entity makes a thorough study of the exchange interaction mechanism in $[Ni(en)_2NO_2]_2(BPh_4)_2$ difficult; however, an interpretation of this difference between dimer and chain may be proposed. We call the z the axis joining the interacting ions in both the dimer and the chain, and we define qualitatively the magnetic orbitals for each of the interacting species as follows. In the dimer, individual nickel complexes are schematized in **1** and **2**; the $(NO_2)^*$ group is common to the

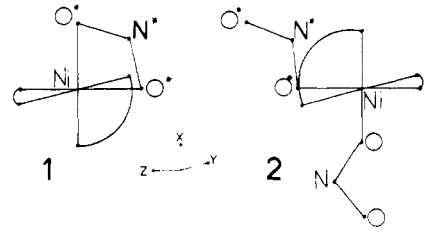

two species with one of the oxygen atoms, close to the z axis, bridging the two metal ions. Each magnetic orbital may be schematically described as resulting from the antibonding interaction between the d_{z^2} or $d_{x^2-y^2}$ metal orbitals and the last occupied molecular orbital of the bridging NO_2^- ligand, i.e., the $6a_1$ MO represented in **3**.[33] The z^2 type magnetic orbitals

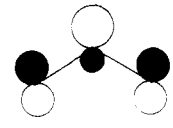

for the species **1** and **2** are shown in **4** and **5**. It is easily seen

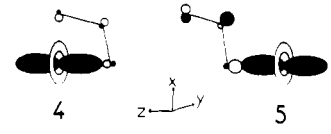

that the d_{z^2}–$6a_1$ interaction in the species **1** is unfavorable. Indeed, the antibonding overlap between the metal and the bridging oxygen atom is partially compensated by the positive overlap along the x axis between the metal and the second oxygen atom of the chelating NO_2 group. In other words, this magnetic orbital will have a weak contribution from the NO_2^- ligand. On the other hand, in the species **2** the orientation of the $(NO_2)^*$ group authorizes a stronger contribution of this ligand to the z^2 type magnetic orbital. As a comparison, we represented in **6** the z^2 type magnetic orbital in the chain,

(27) Capelle, B.; Beauchamp, A.; Dartiguenave, M.; Dartiguenave, Y.; Klein, H. F., Submitted for publication in *Inorg. Chem.* Segal, B. G.; Lippard, S. J. *Inorg. Chem.* **1977**, *16*, 1623. Divaizo, M.; Orlandini, A. B. *J. Chem. Soc., Dalton Trans.* **1972**, 1970.
(28) Ginsberg, A. P.; Martin, R. L.; Brookes, R. W.; Sherwood, R. C. *Inorg. Chem.* **1972**, *11*, 2884.
(29) Meyer, A., unpublished work.
(30) Journaux, Y.; Kahn, O. *J. Chem. Soc., Dalton Trans.* **1979**, 1575.
(31) Stebler, A.; Gudel, H. V.; Furrer, A.; Kjems, J. K. *Inorg. Chem.* **1982**, *21*, 380.
(32) Griffith, J. S. *Struct. Bonding (Berlin)* **1972**, *10*, 87.
(33) Wyatt, J. F.; Hiller, I. H.; Saunders, V. R.; Connor, J. A.; Barber, M. *J. Chem. Phys.* **1971**, *54*, 5311.

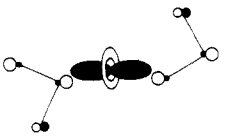

6

which can be largely delocalized toward the NO_2 groups. The $x^2 - y^2$ type magnetic orbital is partially delocalized toward the $(NO_2)^*$ group for the species **1**. This is not true anymore for both the species **2** and the chain. The exchange parameter J experimentally observed may be expressed as the sum of an antiferromagnetic component J_{AF} and a ferromagnetic component J_F. The magniture of J_{AF}, which is here the leading factor, is governed by the overlap integrals $S_{z^2z^2}$ and $S_{x^2-y^2x^2-y^2}$ between magnetic orbitals. $S_{x^2-y^2x^2-y^2}$ is clearly zero for both the dimer and the chain. The relatively weak antiferromagnetic interaction in the dimer with respect to the chain may be simply justified from the schemes **4**, **5**, and **6** by focusing on $S_{z^2z^2}$. Indeed, owing to the weak delocalization of the magnetic orbital shown in **4** toward the chelating NO_2 group, the overlap $S_{z^2z^2}$ is not favored. In the chain, on the contrary, the delocalization on the bridging ligands and the relative orientation of the magnetic orbitals are favorable to give a relatively large $S_{z^2z^2}$ in spite of the Ni–Ni distance.

We are quite conscious that the arguments above are very qualitative and may be even rather rough. However, we believe that we have shown in a simple language the difference between the bridging networks

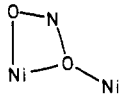

and

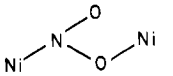

In the former case, the $6a_1$ HOMO of the NO_2^- bridge is not favorably orientated regarding the orientations of the singly occupied orbitals of the Ni(II) ion bound to the two oxygen atoms. In the latter case, in contrast, the $6a_1$ HOMO of the bridge is properly orientated and the antiferromagnetic coupling is more pronounced in spite of the large Ni–Ni distance.

Acknowledgment. This work was technically financially supported by the CNRS, the DGRST, and the DESR.

Supplementary Material Available: Listings of structure factor amplitudes (20 pages). Ordering information is given on any current masthead page.

Contribution from the Consiglio Nazionale delle Ricerche, Rome, Italy, Istituto di Chimica Generale e Inorganica, University of Modena, 41100 Modena, Italy, and Istituto di Chimica, Facoltà di Medicina-Veterinaria, University of Bari, 70126 Bari, Italy

Thermal, Spectroscopic, Magnetic, and Structural Properties of Mixed-Ligand Complexes of Copper(II) with L-Aspartic Acid and Amines. Crystal and Molecular Structure of (L-Aspartato)(imidazole)copper(II) Dihydrate

L. ANTOLINI,[1a] G. MARCOTRIGIANO,[1b] L. MENABUE,[1a] G. C. PELLACANI,*[1a] and M. SALADINI[1a]

Received November 5, 1981

A blue compound of the type Cu(L-Asp)·$2H_2O$ (L-Asp = L-aspartate ion) and its mixed complexes with amine [Cu(L-Asp)B]·xH_2O (B = Im (imidazole), mf (morpholine) and x = 2; B = 2-MeIm (2-methylimidazole) and x = 1; B = py (pyridine), 4-pic (4-methylpyridine) and x = 0) were prepared and characterized by means of thermal, spectroscopic, and magnetic measurements. For one of the mixed complexes, [Cu(L-Asp)(Im)]·$2H_2O$, the crystal structure was also determined by the single-crystal X-ray diffraction method. The compound crystallizes in the orthorhombic space group $P2_12_12_1$ with four formula units in a cell of dimensions a = 16.049 (2) Å, b = 9.622 (1) Å, and c = 7.465 (1) Å. The structure was solved by Patterson and Fourier methods and refined by full-matrix least-squares procedure to a conventional R index of 0.083 for 594 counter data. The structure consists of a polymeric two-dimensional network in which each copper atom is coordinated in a distorted square-pyramidal geometry by three aspartate ions and one imidazole molecule. The aspartate ion acts as a bidentate ligand bridging, in an extended configuration, three metal ions. For [Cu(L-Asp)B]·xH_2O complexes thermal and spectroscopic measurements indicate the presence of distorted square-pyramidal configuration around the copper(II) atoms, similar to that found for the [Cu(L-Asp)(Im)]·$2H_2O$ complex. Their apparently "anomalous" EPR spectra, suggesting a d_{z^2} ground state, are interpreted as due to the presence of magnetically inequivalent sites. For the [Cu(L-Asp)$(H_2O)_2$] and [Cu(L-Asp)(4-pic)] complexes a square-pyramidal configuration tetragonally distorted is tentatively suggested on the basis of their physical measurements.

Introduction

Copper(II) complexes of aspartic acid have received considerable attention, but most of the studies only treat the solution-state behavior.[2] It has been generally suggested that aspartate acts as a tridentate ligand to the same metal ion, while the possibility of polymerization, as found in solid copper(II) glutamate dihydrate, in which the amino acid, in an extended chain conformation, bridges three metal ions,[3] has never been considered. Some other interesting studies in solution regard the mixed-ligand complexes with imidazole or bipyridyl, which seem to enhance the affinity of copper(II) for the oxygen donor sites of anionic ligands,[4,5] and the ternary complexes containing two optically active amino acids with interacting charged group in their side chains.[2,6]

(1) (a) University of Modena. (b) University of Bari.
(2) Evans, C. A.; Guevremont, R.; Rabenstein, D. L. *Met. Ions Biol. Syst.* **1979**, *9*, 41 and references cited therein.
(3) Gramaccioli, C. M.; Marsh, R. E. *Acta Crystallogr.* **1966**, *21*, 594.
(4) Mohan, M. S.; Bancroft, D.; Abbott, E. H. *Inorg. Chem.* **1979**, *18*, 1527.
(5) Sigel, H. *Inorg. Chem.* **1980**, *19*, 1411.
(6) Yamauchi, O.; Odani, A. *J. Am. Chem. Soc.* **1981**, *103*, 391.

0020-1669/82/1321-2263$01.25/0